Cent. Eur. J. Chem. • 7(4) • 2009 • 675-682
DOI: 10.2478/s11532-009-0066-3

VERSITA

Central European Journal of **Chemistry**

# Miniaturization of flow-through generation cells for electrochemical hydride generation in AAS

**Invited Paper**

J. Hraníček*, V. Červený, P. Rychlovský

*Charles University in Prague, Faculty of Science,*
*Department of Analytical Chemistry,*
*Prague 2 CZ 128 43, Czech Republic*

**Received 21 November 2008; Accepted 10 March 2009**

**Abstract:** The construction and optimization of five new types of miniaturized flow-through electrolytic cells with lead cathode and platinum anode for electrochemical hydride generation in atomic absorption spectrometry (HG-QFAAS) were achieved during this research study. The ion-exchange membrane was not part of these cells and only one carrying electrolyte for both electrode chambers was used. Hydride generation efficiency achieved was either comparable or higher than the one recorded for the classic thin-layer generation cell. The inner volume of the cathode chamber was reduced to a quarter of the classic thin-layer flow-through cell. Compared to the commonly used thin-layer flow-through cell, higher sensitivity ($7.32\times10^3$ dm$^3$ $\mu$g$^{-1}$) and better limit of detection (0.32 $\mu$g dm$^{-3}$) were obtained for selenium determination using two of these new generators.

**Keywords:** *Atomic absorption spectrometry • Electrochemical hydride generation • Volatile compounds generation • Hydride generation efficiency • Miniature cells*



## 1. Introduction

Hydride generation is one of the most often used techniques for generation of volatile compounds in atomic spectrometry. A separation of an analyte from the liquid matrix and consequently a reduction of matrix interferences are the most important advantages of this technique [1].

There are two main methods of hydride generation. The one that is used most often is chemical hydride generation (CHG). The other one is electrochemical hydride generation (EcHG); this is an alternative method for generation of volatile compounds [1]. Electrochemical hydride generation eliminates several complications associated with chemical hydride generation. For example, besides using a mineral acid of high purity, a reduction of an analyte a chemical hydride generator requires an unstable and expensive solution of sodium borohydride. Additionally, the reducing agent can contaminate the sample. In an electrochemical hydride generator the electric current is used instead of a reducing agent and therefore the probability of sample contamination is lower.

The thin-layer flow-through electrolytic cells are often used in electrochemical hydride generation technique. They are usually made of Plexiglas, teflon or polypropylene. The cathode and anode chambers are usually separated by an ion-exchange membrane [2-15]. If the Nafion ion-exchange membrane is not used, the chambers can be separated using either a glass frit [16,17] or a ceramic porous tube [18]. Electrodes of different types, shapes and made of variety of materials (lead, carbon or platinum) are fitted in the separated cathode and anode compartments [19,20]. A tubular generator is another design used in electrochemical flow-through cells [18,21]. In these cases the cathode made of porous carbon is fitted in a ceramic porous tube and this tube separates the cathode and anode chambers.

A hydride generator can be used as a derivatization unit between the chromatographic column (HPLC) and the element specific detector [22]. This experimental setup is often used for speciation analysis of hydride forming elements [22]. Both previously mentioned methods – chemical hydride generation

* *E-mail: hranicek.jakub@email.cz*

and electrochemical hydride generation – can be used as the derivatization technique [23]. In case of chemical hydride generation, UV photo-oxidation and pre-reduction steps are necessary for a conversion of the analyte to a suitable form for this technique.

The basic requirement for the arrangement with chromatographic step is minimization of the whole experimental setup. In case of speciation analysis with derivatization step using electrochemical hydride generation, the most critical part of the whole manifold is the electrolytic cell. The inner volume of the generator should be minimized to suppress the analyte zone dispersion. On the other hand, the efficiency of hydride generation should not be decreased by minimization of the inner volume of electrolytic cell. Both of these requirements are contradictory and it is necessary to optimize the construction to achieve the best result.

The aim of this work was construction and optimization of five new types of flow-through electrolytic cells that provide high generation efficiency for electrochemical hydride generation with minimal inner volume and without the use of an ion-exchange separation membrane. These cells can be used in the continuous flow and flow-injection mode of analysis.

## 2. Experimental Procedures

### 2.1. Electrochemical flow-through cells

Five different types of miniaturized flow-through electrolytic cells were constructed (Fig. 1). All of them were made of one piece of Plexiglas in which appropriate electrode chambers were drilled. Each electrode chamber had a thread corresponding to the electrode holder on one side. Electrodes were put into the appropriate chambers of the cell through the electrode holder and tightened using glue. Nafion ion-exchange membrane was not used to separate the chambers. The other difference from the classic thin-layer flow-through cell was the use of only one carrying electrolyte in both chambers. The electrolyte was transported *via* Tygon tubes connected with an inlet and outlet of each of the electrode chambers (it was not the case for cells **A** and **B**). The use of transparent Plexiglas as a construction material enabled visual control of manufacturing of cells and monitoring of hydride generation.

At first, only cells **A** and **B** were constructed (cell **B** was already described in literature [24]). The electrode chambers of these cells were in V-position. A lead-wire cathode was placed in the cathode chamber and a platinum-wire anode in the anode chamber. There was only one electrolyte inlet in the cathode chamber. The electrodes were inserted into these cells from the top. The tips of the electrodes were closer in cell **B** than in cell **A**. Pure electrolyte (or electrolyte containing an analyte) flowed through the inlet into the cell with a constant flow rate and it was distributed into both of the electrode chambers. The gaseous and liquid products from the cathode were transported by the carrier gas (Ar) to the hydrostatic gas-liquid separator. Generated volatile compounds were separated from a liquid matrix and then transported into the externally heated quartz tube atomizer, placed directly in the optical path of the atomic absorption spectrometer (Fig. 2). The temperature of the quartz tube atomizer was 950 °C. The output flow rate from the anode chamber was controlled using a peristaltic pump in such a way that the anode was submerged and the electrolyte mainly flowed through the cathode chamber. Oxygen generated at the platinum anode was carried into waste.

Cells **C** and **D** were constructed later (cell **D** was already described in literature [24]). The electrode

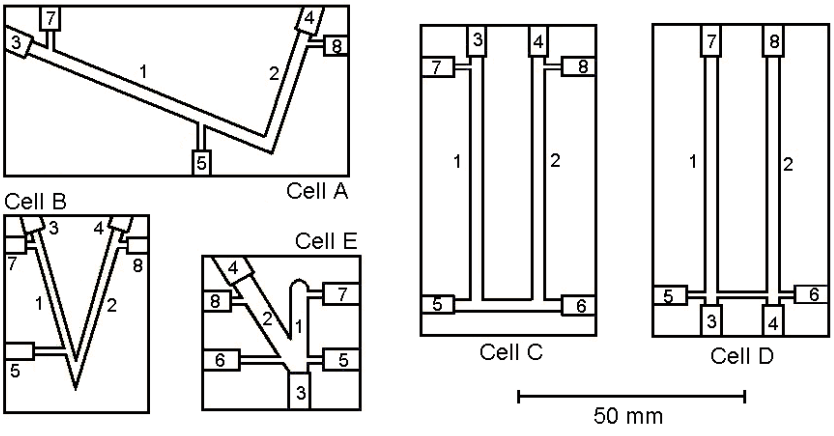


**Figure 1.** New flow-through electrolytic cells: 1 – cathode chamber, 2 – anode chamber, 3 – cathode holder, 4 – anode holder, 5, 6 – electrolyte inlet (pure or containing analyte), 7 – outlet to gas-liquid separator, 8 – waste outlet.

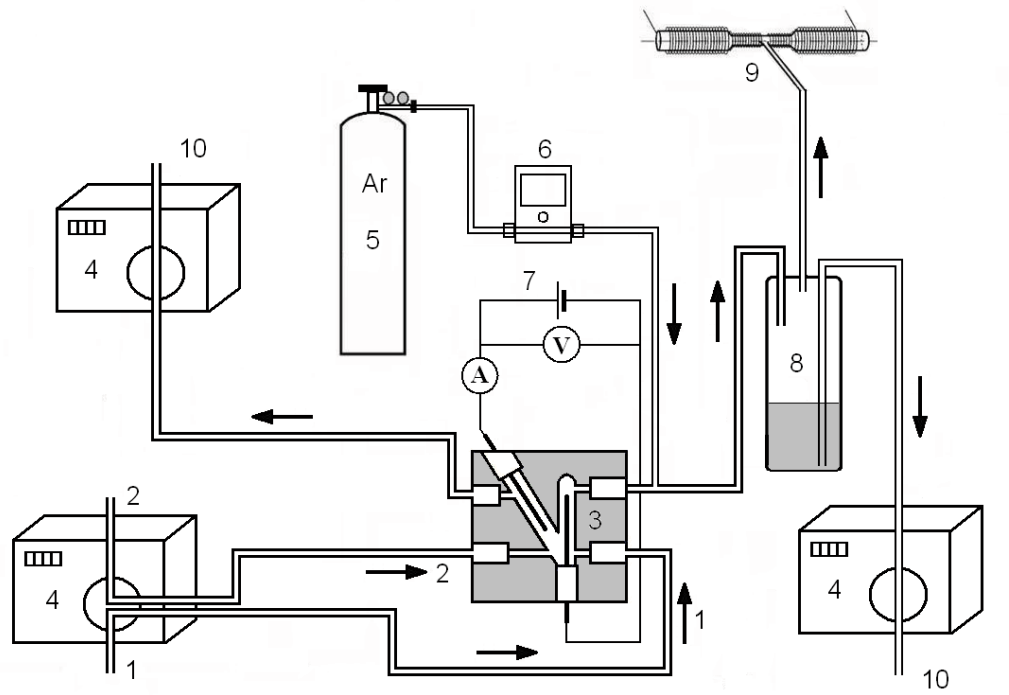


**Figure 2.** Instrumental setup for EcHG-QFAAS with cell **E**: 1 – catholyte, 2 – anolyte, 3 – flow-through electrolyte cell (type E), 4 – peristaltic pump, 5 – carrier gas, 6 – mass flow controller, 7 – electric current supply, 8 – gas-liquid separator, 9 – quartz tube atomizer, 10 - waste

chambers in cells **C** and **D** were parallel, connected by a horizontal coupling. There were two electrolyte inlets in these cells – one to transport pure electrolyte into the anode chamber and the other to transport either pure electrolyte or an electrolyte with the analyte into the cathode chamber. As in cells **A** and **B**, peristaltic pump was used to control the anode output flow rate. The electrodes were inserted from the top of cell **C**-and from the bottom of cell **D**.

Finally, cell **E** was constructed. This cell was a combination of the two previously constructed groups of cells. Cell **E** was the smallest one with miniature electrode chambers in V-position, miniature electrodes and two electrolyte inlets.

Inner volumes of cathode chambers of newly constructed cells (except cell **A**) are summarized in Table 1 (**TL** = common used thin-layer flow-through cell).

## 2.2 Instrumentation

Atomic absorption spectrometer Solaar 939AA (Unicam, UK) with Se hollow cathode lamp (8 mA, 196.0 nm and spectral width 1.0 nm) was used for optimization of working parameters and determination of basic characteristics. Programmable eight channel peristaltic pumps MasterFlex® L/S with mini-cartridge pump head (Cole-Parmer, USA) and Tygon tubes were used for electrolytes transport. Constant electric current supply LPS 303 (American Reliance, Taiwan) with maximal current 3.0 A and maximal voltage 30 V was used for generation of volatile compounds. Teflon tubes (*i.d.* 1.0 mm) with minimal length were used for a connection of all components. Mass flow controller 0–100 mL $min^{-1}$ (Cole-Parmer, USA) was used for to control the carrier gas flow rate. The volume of hydrostatic separator was 6.5 mL. The inner volume of gaseous phase was approximately 1.5 mL.

**Table 1.** Cathode inner volumes and optimal working parameters of used cells.

| Electrolytic cells | D | E | TL | C | B |
|---|---|---|---|---|---|
| Cathode inner volume ($mm^3$) | 214 | 353 | 999 | 339 | 318 |
| Electrode surface area ($mm^2$) | 126 | 29 | 314 | 126 | 117 |
| Generation current (A) | 0.50 | 0.70 | 1.20 | 0.25 | 0.40 |
| Carrier gas flow rate (mL $min^{-1}$) | 10.0 | 20.0 | 20.0 | 10.0 | 10.0 |
| Electrolyte flow rate (mL $min^{-1}$) | 2.5 | 2.5 | 2.0 | 2.0 | 2.5 |
| Electrolyte concentration (mol $dm^{-3}$) | 1 | 1 | 1 | 1 | 1 |
| Anode or withdrawal flow rate (mL $min^{-1}$) | 5.3 | 7.0 | --- | 3.5 | 1.6 |

### 2.3 Reagents

All working selenium (Se (IV)) solutions of required concentration were prepared from the standard (1.000 ± 0.002 g $dm^{-3}$ Se; Analytika, Czech Republic). All electrolytes ($H_2SO_4$, HCl and $H_3PO_4$) were of research grade quality (Merck, Germany). Deionized distilled water prepared with a Milli-QPLUS (Millipore, USA) system was used for all dilution. Ar of the 99.998% purity was used as a carrier gas.

## 3. Results and discussion

Selenium (60 µg $dm^{-3}$) was used as a model solution for optimization of working parameters and testing of new types of flow-through electrolytic cells. Attained sensitivity was chosen in all cases as a comparison criterion. Optimized working parameters and basic characteristics for each tested cell were compared with the commonly used thin-layer flow-through cell. A continuous flow mode was used for most of the experiments. Some experiments were done in a flow injection mode.

### 3.1 Working parameters optimization

Working parameters, including shape and material of the electrode, type and concentration of the electrolyte, rate of flow of the electrolyte and the carrier gas, the generation current, the rate of withdrawal flow from the anode chamber *etc*., were optimized for each newly constructed cell.

At first, cell **A** was tested. Technical problems of construction of new cells were eliminated during this test. The first encountered problem was a balance of electrolyte inside the cell. In comparison with the conventional thin-layer electrolytic cell there was no Nafion ion-exchange membrane and the electrolyte flowed freely from one electrode chamber to the other. In order to obtain high generation efficiency it was necessary to ensure that the electrolyte with the analyte flowed directly through the cathode chamber (valid for cells **A** and **B**). The volatile compounds and other products of cathode reaction were moved into the gas-liquid separator only if there was a definite overpressure in the cathode chamber. The cathode and anode chambers were connected together and therefore it was necessary to set up the overpressure by peristaltic pump behind the outlet of anode chamber. The output flow rate was set up in such a way that the anode was always submerged and only gaseous products of anodic reaction were transported into the waste.

A flow rate in the anode chamber was also optimized for the other cells. It was necessary to establish a hydrostatic balance between the influent electrolyte, effluent electrolyte and gaseous products formed during electrode reactions by using peristaltic pump that controlled the anodic output flow rate. If the anode flow rate was too low, the electrolyte was forced out of the anode chamber by gaseous products and if the electrolyte level sank under the bottom of the electrode, the electrolysis was discontinued. If the anode flow rate was too high, the same situation was observed in the cathode chamber. To ensure continuous electrolysis in the electrolytic cells, it was necessary to find the optimized anode flow rate (different for each cell) (Fig. 3).

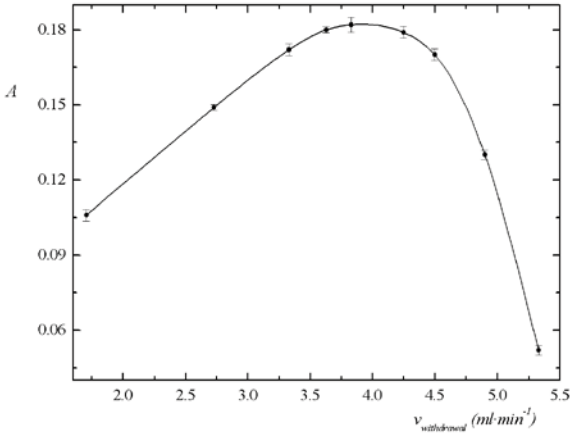


**Figure 3.** The dependence of the absorption signal on withdrawal flow rate for cell **D**: I = 0.25 A, $v_{Ar}$ = 10 mL $min^{-1}$, $v_{el}$ = 2.0 mL $min^{-1}$, $c_{el}$ = 1 mol $dm^{-3}$, $c_{Se}$ = 60 µg $dm^{-3}$.

In general, for cells **A**, **B** and **E** the length of the cathode or the anode should be less than the distance from the electrode base to the electrolyte inlet to the cathode (anode) chamber. If the electrode is too long, the gaseous products from the electrode break the liquid column and the electrolysis is stopped. The electrode chambers in cells **C** and **D** were connected by a horizontal conjunction of a small diameter. The effect of gaseous bubbles was very significant for these cells, especially for cell **C**. There were two reasons why gaseous bubbles appeared in the horizontal tube. Firstly those gaseous bubbles appeared if the air was sucked in when the pure electrolyte and the electrolyte containing the analyte were exchanged. The distance between the tips of electrodes was critical for the maximal value of the generation current used to ensure continuous electrolysis. When these tips were farther apart, it was necessary to use a higher electric voltage and the electrolyte was getting warm and finally boiled. That

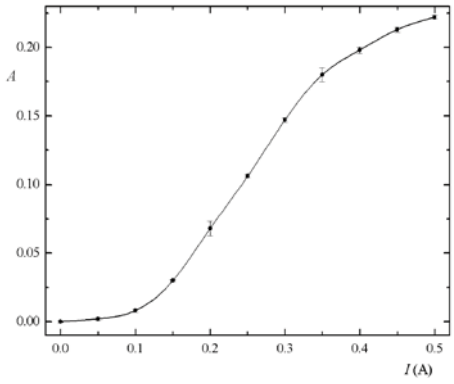


**Figure 4.** The dependence of absorption signal on the generation current for cell **B**: $c_{el}$ = 1 mol dm$^{-3}$, $v_{Ar}$ = 10 mL min$^{-1}$, $v_{el}$ = 2.5 mL min$^{-1}$, $c_{Se}$ = 60 $\mu$g dm$^{-3}$.

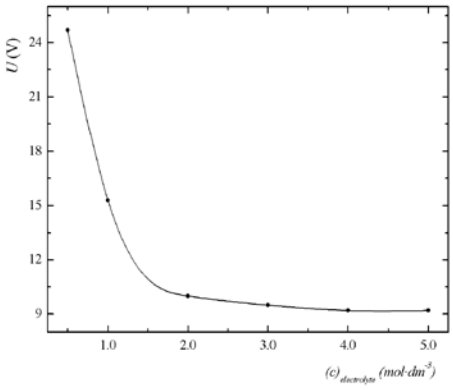


**Figure 5.** The dependence of the applied electric voltage on electrolyte concentration for cell **D**: I = 0.3 A, $v_{Ar}$ = 10.0 mL min$^{-1}$, $v_{el}$ = 2.5 mL min$^{-1}$, $v_{od}$ = 3.8 mL min$^{-1}$, $c_{Se}$ = 60 $\mu$g dm$^{-3}$

was the other reason why gaseous bubbles appeared in the horizontal tube.

The dependence of the absorption signal on the flow rate of the electrolyte flowing into the cells was not very significant. These flow rate values had only lower limit if electrolysis was interrupted because of insufficient transport of the electrolyte into the cell. To establish a balance between the influent and effluent electrolyte and the gaseous and liquid products, the optimal flow rate of the influent electrolyte was found and consequently the withdrawal flow rate in the anode chamber was optimized.

Obviously it was necessary to choose an optimal electrolyte. When HCl (typical electrolyte used in conventional thin-layer cells) was used as an electrolyte, there was zero or minimal signal observed for different concentrations of selenium solution. The reason why such a small signal was observed was probably gaseous chlorine generated on the anode surface. The chlorine was consequently infiltrated into the cathode chamber and interfered with generated selenium hydride. When $H_3PO_4$ was tested as an electrolyte the result was also a very small absorption signal. Finally, $H_2SO_4$ of concentration 1.0 mol dm$^{-3}$ was used for all further experiments.

Because of a minimal inner volume and the problems with gaseous bubbles in these cells it was impossible to introduce a carrier gas (Ar) in front of the inlet into the cell as bubbles of carrier gas often interrupted the electrolysis. Due to this fact, it was necessary to introduce the carrier gas in between the cell output and the gas-liquid separator. The releasing of hydride from the cathode surface was very successful and the carrier gas was used only for speeding up the transport of selenium hydride to the quartz atomizer. In a conventional thin-layer electrolytic cell, the carrier gas was used for better hydride releasing from the cathode surface and for the transport of hydride to the atomizer.

Typical optimal carrier gas flow rates were in the range of 10.0 to 20.0 mL min$^{-1}$. In absence of carrier gas the released hydride was transported into the atomizer only by hydrogen simultaneously released on the cathode surface and the accrual of a signal because of the very small change of the analyte concentration. The highest sensitivity was observed when the flow rate of the carrier gas was near the optimal value. The sensitivity decreased when the flow rates were higher than optimal; it was due to increased convection inside the quartz tube atomizer which caused a decrease in the concentration of free atoms of the analyte.

The dependence of the attained sensitivity on the generation current had characteristic shape of the curve for each electrolytic cell (Fig. 4). For low generation current values small absorption signals were obtained. For the current of 0.15 to 0.35 A (for cell **B**) the signal upraised and for the current of more than 0.35 A the signal increased gradually. For continuous hydride generation it is better to use the current of value lower than the maximal one because the lifetime of the generation cells is prolonged.

Finally, the concentration of the electrolyte ($H_2SO_4$) was optimized. The curve of the dependence of the absorption signal on the electrolyte concentration is decreasing all over its range. This might lead to a conclusion that very low concentration of the electrolyte should be used in order to obtain signals of high intensity. But if a low concentration of the electrolyte is used the concentration of particles that are able to conduct electric

**Table 2.** Basic characteristics of Se determination.

| Electrolyte cells | D | E | TL | C | B |
|---|---|---|---|---|---|
| Limit of detection ($\mu$g dm$^{-3}$) | 0.32 | 0.52 | 0.60 | 1.50 | 2.23 |
| Limit of determination ($\mu$g dm$^{-3}$) | 1.06 | 1.73 | 2.01 | 5.20 | 7.44 |
| Sensitivity $\times$ 10$^3$ (dm$^3$ $\mu$g$^{-1}$) | 7.32 | 4.14 | 4.86 | 2.76 | 1.53 |
| Repeatability (%) | 0.56 | 0.53 | 0.62 | 1.78 | 1.40 |
| Correlation coefficient | 0.9988 | 0.9992 | 0.9995 | 0.9985 | 0.9982 |
| Linear dynamic range ($\mu$g dm$^{-3}$) | 1.06-100 | 1.73-100 | 2.01-100 | 5.20-100 | 7.44-100 |

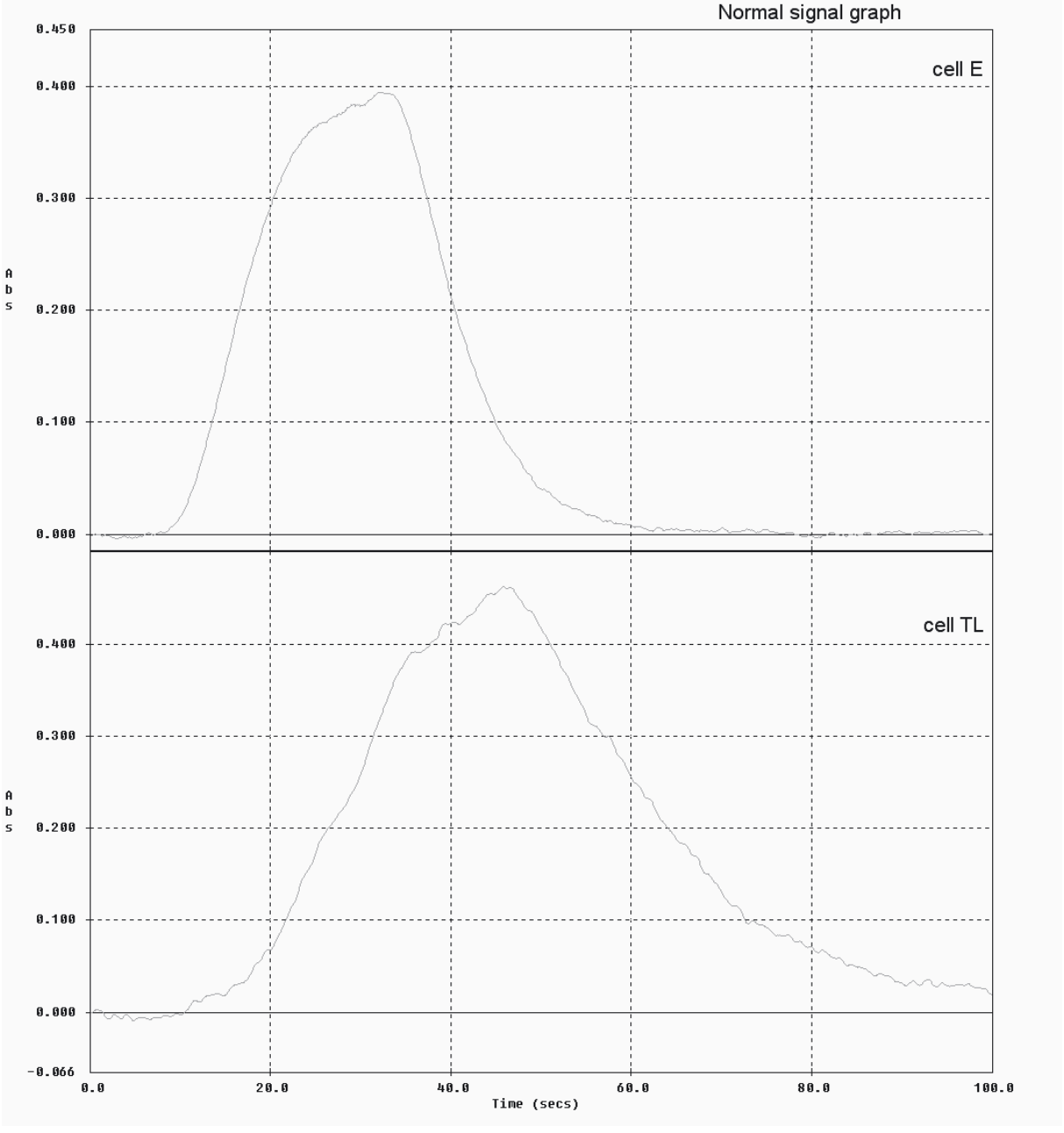


**Figure 6.** Time dependence of absorbance signal for cells **E** and **TL** in FIA mode: I = 0.7 A (cell **E**) or 1.2 A (cell **TL**), $v_{Ar}$ = 20.0 mL min$^{-1}$, $v_{el}$ = 2.0 mL min$^{-1}$, $c_{Se}$ = 100 $\mu$g dm$^{-3}$, $c_{el}$ = 1 mol dm$^{-3}$, injected volume 1000 $\mu$L.

**Table 3.** Characteristics of FIA signal for each cell.

| Electrolytic cells | TL | B | C | D | E |
|---|---|---|---|---|---|
| $t_r$ (s) | 12 | 25 | 23 | 12 | 8 |
| $t_{max}$ (s) | 47 | 50 | 45 | 48 | 36 |
| $A_{max}$ | 0.455 | 0.150 | 0.290 | 0.750 | 0.396 |
| $A_{60}$ | 0.253 | 0.125 | 0.240 | 0.400 | 0.012 |
| rel. $A_{60}$ (%) | 55.60 | 83.33 | 82.76 | 53.33 | 3.03 |
| $A_{80}$ | 0.072 | 0.060 | 0.110 | 0.150 | 0.001 |
| rel. $A_{80}$ (%) | 15.82 | 40.00 | 37.93 | 20.00 | 0.25 |

$t_r$ - *time of first signal change detected*
$t_{max}$ - *time of maximal signal*
$A_{max}$ - *maximal absorbance*
$A_{60}$ - *absorbance t = 60 s*
$A_{80}$ - *absorbance t = 80 s*
*rel. A* - *relative absorbance for each cell*

current is low and it is necessary to use high electric voltage which causes the electrolyte to warm up. This is why it is better to use a higher electrolyte concentration combined with higher electric current to achieve higher generation efficiency. The electric voltage that is used to keep the electric current constant is dependent on the resistance of the electrolyte and on the length of the electrode tip. The dependence of loaded electric voltage on the electrolyte concentration is shown in Fig. 5.

The optimal working parameters and the inner volumes of all cells are given in Table 1 and are compared to the conventional thin-layer electrolytic cell (**TL**).

In the new constructed cells, the inner volume is several times less than in the conventional thin-layer electrolytic cell. Another typical feature of the new cells is lower generation current necessary for obtaining a signal comparable to the signal for cell **TL**.

### 3.2 Basic characteristics of selenium determination by EcHG-QFAAS using new types of electrolytic cells

Using optimal working parameters, the calibration curves for low (0 - 20 μg $dm^{-3}$) and high (0-250 μg $dm^{-3}$) concentrations were measured for cells **B**, **C**, **D**, **E** and cell **TL** for selenium determination. Cell A was not suitable for selenium determination because of low generation efficiency. Together with this calibration, the long-term stability of absorption signal corresponding to the specific concentration of the analyte was measured.

Basic characteristics of selenium determination, including limit of detection, limit of determination, sensitivity, repeatability, correlation coefficient, linear dynamic range and other parameters, were obtained by processing these calibrations. For summary of these characteristics see Table 2.

### 3.3 Flow injection mode

All new constructed electrolytic cells were tested in a FIA mode. The speed of signal response dependent on the analyte concentration change was tested. The same electrolyte flow rate, 2.0 mL $min^{-1}$, was used for each cell. The solution of the concentration of 100 μg $dm^{-3}$ Se was batched for the duration of 30 s (corresponding injected volume of Se solution 1 mL). The same experimental conditions were used for each new cell for comparison with the cell **TL**. Other parameters were concurrent with optimal working parameters. Only for cell **E** (with very small inner volume), symmetric peak without marked dispersion was obtained (Fig. 6).

Basic characteristics of FIA signals are summarized in Table 3. The lowest time of maximal absorption signal is duly obtained for cell E. In this cell, the absorption signal value has only 3.03% of maximal absorption signal after 60 s. Comparison of a FIA signal for cell **E** and **TL** is shown in Fig. 6.

## 4. Conclusion

Five new designs of flow-through electrolytic cells were constructed and tested. These electrolytic cells were able to provide sensitivity either comparable or higher and lower concentration detection limit in comparison with the original thin-layer cell at markedly lower generation electric current values. Compared with the commonly used thin-layer flow-through cell, the higher sensitivity ($7.32\times10^3$ $dm^3$ $\mu g^{-1}$) and better limit of detection (0.32 μg $dm^{-3}$) were obtained for selenium determination using two of these new generators (cells **D** and **E**). Concentration detection limits obtained by cells **D** and **E** for selenium determination with direct detection HG-AAS are comparable or markedly lower than some authors mention (0.62–17 μg $dm^{-3}$) [2,3,11,18,25,26].

Thanks to their lower inner volumes (a quarter of the volume in the original thin-layer flow-through cell) and minimal signal zone dispersion (especially for cell **E**) compared with the commonly used thin-layer flow-through cell, it is possible to use these miniaturized cells as derivatization units after HPLC separation in speciation analysis.

## Acknowledgment

The authors thank the Grant Agency of the ASCR (project: A400310507/2005) and MSMT CR (research project: MSM0021620857) for the financial support.

## References

[1] J. Dědina, D. Tsalev, Hydride Generation Atomic Absorption Spectrometry (Wiley, Chichester, 1995)
[2] Y.H. Lin, X.R. Wang, D.X. Yuan, P.Y. Yang, B.L. Huang, Z.X. Zhuang, J. Anal. Atom. Spectrom. 7, 287 (1992)
[3] L. Brockmann, C. Nonn, A. Golloch, J. Anal. Atom. Spectrom. 8, 397 (1993)
[4] D.M. Hueber, J.D. Winefordner, Anal. Chim. Acta 316, 129 (1995)
[5] J. Šíma, P. Rychlovský, Chem. Listy 92, 676 (1998) (in Czech)
[6] W.W. Ding, R.E. Sturgeon, J. Anal. At. Spectrom. 11, 225 (1996)
[7] W.W. Ding, R.E. Sturgeon, Spectrochim. Acta, Part B 51, 1325 (1996)
[8] E. Denkhaus, A. Golloch, T.U. Kampen, M. Nierfeld, U. Telgheder, Fresenius J. Anal. Chem. 361, 733 (1998)
[9] C. Schickling, J.F. Yang, J.A.C. Broekaert, J. Anal. At. Spectrom. 11, 739 (1996)
[10] L.F. Machado, A.O. Jacintho, A.A. Menegario, E.A. Zagatto, M.F. Gine, J. Anal. At. Spectrom. 13, 1343 (1998)
[11] U. Pyell, A. Dworschak, F. Nitschke, B. Neidhart, Fresenius J. Anal. Chem. 363, 495 (1999)
[12] J. Šíma, P. Rychlovský, J. Dědina, Spectrochim. Acta, Part B 59, 125 (2004)
[13] J.Šíma, P. Rychlovský, Spectrochim. Acta, Part B 58, 919 (2003)
[14] V. Červený, P. Rychlovský, J. Netolická, J. Šíma, Spectrochim. Acta, Part B 62, 317 (2007)
[15] W. Zhang, W. Gan, X. Lin, Anal. Chim. Acta 539, 335 (2005)
[16] D. Schaumlöffel, B. Neidhart, Fresenius J. Anal. Chem. 354, 866 (1996)
[17] D.M. Hueber, J.D. Winefordner, Anal. Chim. Acta 316, 129 (1995)
[18] F. Laborda, E. Bolea, J.R. Castillo, J. Anal. At. Spectrom. 15, 103 (2000)
[19] E. Denkhaus, A. Golloch, X.M. Guo, B. Huang, J. Anal. Atom. Spectrom, 16, 870 (2001)
[20] F. Laborda, E. Bolea, J.R. Castillo, Anal. Bioanal. Chem. 388, 743 (2007)
[21] B. Ozmena, F.M. Matysika, N.H. Bings, J.A.C. Broekaert, Spectrochim. Acta, Part B 59, 941 (2004)
[22] D.L. Tsalev, J. Anal. At. Spectrom. 14, 147 (1999)
[23] V. Červený, P. Rychlovský, In: S. Ružičková (Ed.), XVIIth Slovak Spectroscopic conference, 5-9 Sep. 2004, The High Tatras - Tatranské Zruby, Slovakia (Technical University Košice, Košice, 2004)
[24] J. Hraníček, V. Červený, P. Rychlovský, Chem. Listy 102, 200 (2008) (in Czech)
[25] L.F. Machado, A.O. Jacintho, M.F. Gine, Química Nova 23, 30 (2000)
[26] E. Bolea, F. Laborda, J.R. Castillo, Anal. Sci. 19, 367 (2003)